

**Numerical analysis of polymer diffusiophoresis by means of the molecular dynamics**S.Ramírez-Hinestrosa,<sup>1</sup> H. Yoshida,<sup>2,3</sup> L. Bocquet,<sup>2</sup> and D. Frenkel<sup>1, a)</sup><sup>1)</sup>*Department of Chemistry, University of Cambridge, Lensfield Road,  
Cambridge CB2 1EW, United Kingdom*<sup>2)</sup>*LPS, UMR CNRS 8550, École Normale Supérieure, 24 rue Lhomond, 75005 Paris,  
France*<sup>3)</sup>*Toyota Central R&D Labs., Inc., Bunkyo-ku, Tokyo 112-0004,  
Japan*

(Dated: 17 May 2022)

We report a numerical study of the diffusiophoresis of short polymers using non-equilibrium molecular dynamics simulations. More precisely, we consider polymer chains in a fluid containing a solute which has a concentration gradient, and examine the variation of the induced diffusiophoretic velocity of the polymer chains as the interaction between the monomer and the solute is varied. We find that there is a non-monotonic relation between the diffusiophoretic mobility and the strength of the monomer-solute interaction. In addition we find a weak dependence of the mobility on the length of the polymer chain, which shows clear difference from the diffusiophoresis of a solid particle. Interestingly, the hydrodynamic flow through the polymer is much less screened than for pressure driven flows.

---

<sup>a)</sup>Electronic mail: df246@cam.ac.uk

## I. INTRODUCTION

In a bulk fluid, concentration gradients cannot cause fluid flow. However, a gradient in the chemical potential of the various components in a fluid mixture, can cause a net hydrodynamic flow in the presence of an interface that interacts differently with the different components of the mixture. Such flow induced by chemical potential gradients is usually referred as diffusio-osmosis (see e.g.<sup>1</sup>). The same mechanism that causes diffusio-osmosis can also drive the motion of a colloid, or other mesoscopic moiety, under the influence of chemical potential gradients in embedding fluid. Clearly, if the mesoscopic particle (say a colloid) is very large compared to the characteristic length scale on which adsorption or depletion occurs, it is reasonable to use the Derjaguin approximation<sup>2,3</sup>, i.e. to describe the colloid-fluid interface as locally flat, and thus estimate the speed of diffusiophoresis. However, the Derjaguin approach is likely to fail if the particles that are subject to phoresis are no longer large compared to the range of adsorption/depletion. There is yet another situation where the Derjaguin approach is obviously questionable, namely in the case of particles that do not have a well-defined surface. One particularly important example is the case of diffusiophoresis of polymers: molecules that have a fluctuating shape and an intrinsically fuzzy surface. One manifestation of this fuzziness is the fact that the magnitude of the Kirkwood approximation for the hydrodynamic radius  $R_h$  of a long self-avoiding polymer is about 63% of the radius of gyration  $R_g$ <sup>4</sup>: for a smooth sphere, this ratio would be  $\approx 107\%$  (the Kirkwood expression for  $R_h$  is only an approximation: the point is that the averages are different and that hydrodynamic radius is smaller than for a corresponding solid object). This difference implies that the density inhomogeneity of a self-avoiding polymer results in penetration of hydrodynamic flow fields into its outer “fuzzy” layer. In addition, solutes can diffuse through the polymer. This fuzziness clearly makes it difficult to describe a polymer as a solid sphere surrounded with pure liquid, and hence a Derjaguin approach is questionable. The lack of predictive power of the colloidal approximation was pointed out previously by experiments with  $\lambda$ -DNA by Palacci et al<sup>5,6</sup>.

There is another factor that makes diffusiophoresis of polymers unusual: since the driving force for diffusiophoresis comes from an excess (or deficit) of solute in the fluid surrounding the polymer, the stronger a solute is attracted to a polymer, the larger this excess will be. However, a strongly binding solute may result in the collapse of the polymer to a compact globule (scaling exponent 1/3). Hence, unlike in the case of colloids, one cannot assume that the size of polymers subject to diffusiophoresis is independent of the polymer-solute interaction. Furthermore, a so-

lute excess/deficit may not be sufficient for the occurrence of diffusiophoresis: if the solutes are strongly adsorbed onto the polymer, they become effectively immobile relative to the polymer, in which case the excess/deficit do not contribute to diffusiophoresis.

In this paper, we report systematic molecular dynamic simulations of diffusiophoretic transport of short polymers. Specifically, we apply non-equilibrium molecular dynamic simulations using a microscopic force acting on each species, and examine the effect of interaction parameters between the monomer and the solute on the induced diffusiophoretic velocity of the polymer. Our simulations indeed reveal a non-monotonic dependence of the phoretic mobility  $\Gamma_{ps}$  on  $\epsilon_{ms}$ , the interaction strength between the polymer and solute. We have investigated the influence of the size of the polymer on its diffusiophoretic mobility. We find a weak polymer-size dependence of the mobility. We compare these findings with the corresponding theoretical predictions for a colloidal particle.

## II. THERMODYNAMICS FORCES AND THEIR MICROSCOPIC REPRESENTATION

Conceptually the most straightforward way of simulating diffusiophoresis would be to carry out a Non-Equilibrium Molecular Dynamics (NEMD) simulation with an imposed concentration gradient, following a procedure similar to Thompson et al<sup>7</sup>. Nonetheless, there are several drawbacks associated with this approach for modeling diffusiophoresis, the most significant being that periodic boundary conditions are incompatible with the existence of constant concentration gradients. However, in analogy with simulations of systems in homogeneous electrical fields, we can replace the gradient of a chemical potential by an equivalent force per particle that can be kept constant, and therefore compatible with periodic boundary conditions<sup>8,9</sup>. This field-driven non-equilibrium approach has been often applied in other contexts<sup>10</sup>. The idea is to impose a mechanical constraint (i.e an external field) that mimics the effect of the force<sup>11</sup>. To see how this approach works in the systems that we study, we first consider diffusio-osmosis in a binary mixture of solvent ( $f$ ) and solute ( $s$ ) particles, which are subjected to a gradient of chemical potential of one of the species (e.g.  $s$ ), and a gradient in the pressure (in bulk fluids in the absence of external body forces, the pressure gradient will typically vanish). We assume that the system is at constant temperature. Adjari<sup>12</sup> derived an expression for the transport matrix  $\Gamma$  that relates the fluxes, viz. the total volume flow  $\mathbf{Q}$  and the excess solute flux  $\mathbf{J}_s - c_s^B \mathbf{Q}$ , with the gradient of pressure  $-\nabla P$  and the gradient of the

chemical potential of one of the species. There are only two independent thermodynamic driving forces as, at constant temperature, only two of the three quantities  $\nabla P$ , the solute  $\nabla\mu_s$  and the solvent  $\nabla\mu_f$  are independent. In fact, it is convenient to define a slightly modified chemical potential gradient  $\nabla\mu'_s$  by  $\nabla\mu'_s \equiv [1 + c_s^B/c_f^B]\nabla\mu_s$ . With this definition, the linear transport equations can be written as

$$\begin{bmatrix} \mathbf{Q} \\ \mathbf{J}_s - c_s^B \mathbf{Q} \end{bmatrix} = \begin{bmatrix} \Gamma_{qq} & \Gamma_{qs} \\ \Gamma_{sq} & \Gamma_{ss} \end{bmatrix} \begin{bmatrix} -\nabla P \\ -\nabla\mu'_s \end{bmatrix}, \quad (1)$$

where  $\Gamma_{ij}$ 's are the Onsager transport coefficients connecting the different fluxes with the thermodynamic driving forces. In what follows, it is convenient to replace  $\nabla\mu_i$  the gradient of the chemical potential on species  $i$  by an equivalent external force  $\mathbf{F}_i^\mu$  (see<sup>8</sup>).

Having considered the case of a binary solvent-solute mixture, we now add a third component, namely the polymer, to the system. Again, not all chemical potential gradients are independent, as it follows from the Gibbs-Duhem equation that (at constant temperature):

$$VdP = SdT + \sum_i N_i d\mu_i. \quad (2)$$

In what follows, we will consider bulk fluids, in which case pressure and thermal gradients are absent, so we can write:

$$\mathbf{F}_p = -(\mathbf{F}_s^\mu N_s + \mathbf{F}_f^\mu N_f), \quad (3)$$

where  $\mathbf{F}_p$  denotes the equivalent force on the polymer due to  $\nabla\mu_p$ . This equation simply expresses the fact that there can be no net external force on the fluid: if there were, the system would accelerate without bound, as there are no walls or other momentum sinks in the system. In simulations, it is convenient to work with a force per monomer, rather than a force on the center-of-mass of the polymer:  $\mathbf{F}_m = \mathbf{F}_p^\mu/N_m$ . Equation (3) establishes a connection between all chemical potential gradients (or the corresponding microscopic forces), which must be balanced throughout the system as phoretic flow cannot cause bulk flow.

We will now compute the rate of polymer diffusiophoresis using Eq. (3) as our starting point.

### III. MOLECULAR DYNAMICS (MD) SIMULATIONS

We performed non-equilibrium Molecular Dynamics (NEMD) simulations using LAMMPS<sup>13</sup>. In most simulations, particles interact via a 12-6 Lennard-Jones potential (LJ)  $V_{LJ}(r) = 4\epsilon_{ij}^{LJ}[(\sigma_{ij}^{LJ}/r)^{12} -$

$(\sigma_{ij}^{LJ}/r)^6]$  shifted and truncated at  $r = r_c$ , such that

$$V_{TS}(r) = \begin{cases} V_{LJ}(r) - V_{LJ}(r_c), & \text{if } r \leq r_c \\ 0, & \text{otherwise.} \end{cases} \quad (4)$$

The indices  $i$  and  $j$  denote the particle types in our simulations: solutes ( $s$ ), solvents ( $f$ ) and monomers ( $m$ ). To keep the model as simple as possible, we assume the same Lennard-Jones interaction for the particle pairs  $ss$ ,  $sf$ ,  $ff$  and  $mf$  with  $\epsilon_{ij}^{LJ} = \epsilon_0$  and  $\sigma_{ij}^{LJ} = \sigma_0$ . However, the solute-monomer interaction strength  $\epsilon_{sm}^{LJ}$  was varied to control the degree of solute adsorption or depletion around the polymer. Yet, we kept  $\sigma_{sm}^{LJ}$  equal to  $\sigma_0$ . For the monomer-monomer interaction, we use a purely repulsive Weeks-Chandler-Andersen potential<sup>14</sup>, i.e. a Lennard-Jones potential truncated and shifted at the minimum of the LJ potential,  $r_c = 2^{1/6}\sigma_0$ . For all other interactions,  $r_c = 2.5\sigma_0$ . Finally, neighboring monomers are connected by a finite extensible, nonlinear elastic (FENE) anharmonic potential  $U_{FENE}(r)$ ,<sup>15,16</sup>

$$U_{FENE}(r) = -\frac{kR_0^2}{2} \ln \left[ 1 - \left( \frac{r}{R_0} \right)^2 \right], \quad (5)$$

with  $k = 7\epsilon_0/\sigma_0^2$  and  $R_0 = 2\sigma_0$ . In what follows, we use the mass  $m_0$  of all the particles ( $s, f$  and  $m$ ) as our unit of mass and we set our unit of energy equal to  $\epsilon_0$ , whilst our unit of length is equal to  $\sigma_0$ . As a result, forces are expressed in units  $\epsilon_0/\sigma_0$ , and our unit of time is  $\tau \equiv \sigma_0\sqrt{m_0/\epsilon_0}$ .

## A. Equilibration

We studied the diffusiophoresis of a single polymer chain composed of 30 monomers,  $N_m = 30$ , suspended in a binary fluid mixture. The initial simulation box dimensions were  $L_x = 20\sigma_0$ ,  $L_y = 20\sigma_0$ ,  $L_z = 30\sigma_0$  and the number of fluid particles was 8748. After equilibration, chemical potential gradients were applied along the  $x$ -axis. We distinguished two types of regions in the simulation box: one slab with width  $20\sigma_0$  in the  $z$ -direction, and periodically repeated in  $x$  and  $y$ , was centred around the polymer. The other two slabs, with height  $10\sigma_0$  each, contained only bulk fluid (see Fig 1).

Our aim was to carry out simulations under conditions where the composition of the bulk fluid was kept fixed, even as we varied the monomer-solute interaction. Moreover, we prepared all systems at the same hydrostatic pressure.

Fixing the bulk concentration of the liquid requires careful equilibration, in particular in cases where the solute binds strongly to the polymer. As this process would deplete solute from the rest of the system, it is necessary to readjust the solute concentration in the bulk.

The system was originally prepared with a homogeneous solvent-solute distribution. During equilibration there is a flux of solutes towards the polymer. This inward flux depletes solutes from the bulk region. To keep the bulk solute concentration fixed and, at the same time fix the the pressure, we performed NPT simulations using a Nosé-Hoover thermostat/barostat<sup>17</sup>. The equations of motion were integrated using a velocity-Verlet algorithm with time step  $\Delta t = 0.005\tau$ . After the relaxation of the initial configuration, the box was allowed to fluctuate in the  $y$  direction, fixing  $T = 1.0$  and  $P = 1.0$  for  $2 \times 10^4$  steps. In the meantime, to keep the bulk concentration constant whilst adsorbing (or expelling) solutes around the polymer, we attempted to swap solvent and solute molecules  $10^4$  times for each MD step throughout the simulation box. In addition, we swapped particles identities in the bulk every 200 steps so as to maintain the bulk solute concentration  $c_s^B \approx 0.376$ . After this preparation,  $L_y$  was fixed and the particle swaps/exchanges were stopped. We then carried out a run of the last  $10^5$  steps, at constant  $NVT$ . This last step concluded the equilibration without an applied field.

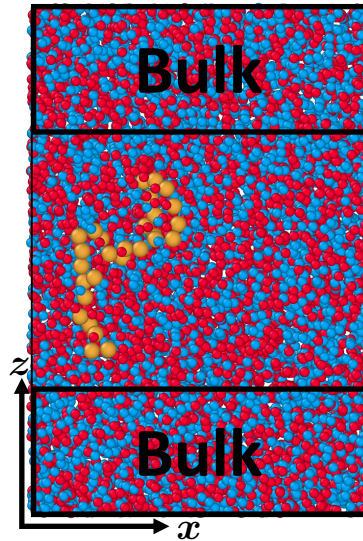


FIG. 1: Simulation box showing solutes (red), solvents (blue) and monomers (orange). The bulk regions are shown inside black boxes. In the bulk, the solute and solvent concentrations are unperturbed by the presence of the polymer.

## B. Field-driven simulation

Having prepared a system of polymer in a fluid mixture with a pre-determined pressure and bulk composition, we now consider the effect of chemical potential gradients on the phoretic motion of the polymer. As discussed above, we represent the chemical potential gradients by equivalent external forces that are compatible with the periodic boundary conditions. Importantly, the forces should be chosen such that a) there is no net force on the system as a whole and b) there is no net force on the bulk solution away from the polymer. These conditions imply that there is only one independent force that can be varied. In the present case, we chose to vary the force on the solute  $F_s^\mu$ , which was varied between 0 and  $0.1 \epsilon_0/\sigma_0$ . During all the field-driven simulations, we constrained the  $z$ -coordinate of the center of mass of the polymer to be in the center of the simulation box, thus ensuring that the “bulk” region is not perturbed by its presence. Having specified the force on the solute, the force on the solvent particles follows from mechanical equilibrium in the bulk (see Fig. 1):

$$\mathbf{F}_s^\mu N_s^B + \mathbf{F}_f^\mu N_f^B = 0, \quad (6)$$

where  $N_s^B$ ,  $N_f^B$  denote the number of solutes and solvent in the bulk region. Once the forces in the bulk have been specified, the phoretic force on the polymer  $\mathbf{F}_p^\mu$  is obtained by imposing force balance on the system as a whole (Eq. (3)).

## IV. RESULTS AND DISCUSSION

### A. Phoretic velocity

In Fig 2 the polymer velocities in the direction of the gradient  $v_p^x$  are plotted for three different pair of LJ parameters. When there is adsorption of solutes around the polymer ( $\epsilon_{sm}^{LJ} = 1.5$ ), the polymer follows the gradient, migrating towards regions where the solute concentration is higher. Conversely, when there is depletion ( $\epsilon_{sm}^{LJ} = 0.5$ ) the polymer will move in the opposite direction. As a null check, we also performed simulations for the case where the  $\epsilon_{ms}^{LJ} = \epsilon_{mf}^{LJ}$ . In that case, there should be no phoresis, as is indeed found in the data shown in Fig. 2. The figure also shows that our simulations appear to be in the linear regime, as the magnitude of the phoretic velocity increases linearly with the strength of the applied field.

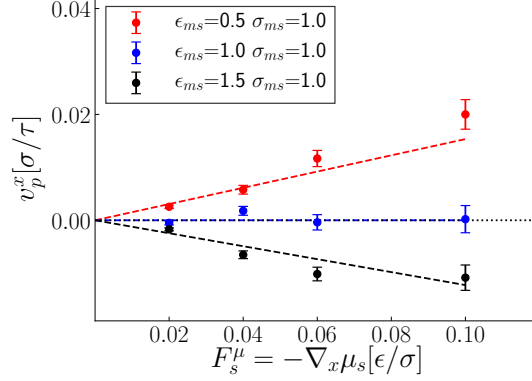


FIG. 2: Polymer velocities in the direction of the gradient for different LJ interactions  $(\epsilon_{ms}^{LJ}, \sigma_{ms}^{LJ})$  vs the force applied on the solute particles.

## B. Mobility dependence on the interaction

The mobility  $\Gamma_{ps}$  of a polymer moving under the influence of a gradient in the solute chemical potential is defined through:

$$v_p^x = \Gamma_{ps} \nabla_x \mu_s. \quad (7)$$

We can compute  $\Gamma_{ps}$  as a function of the polymer-solute interaction strength from the slope of the  $v_p^x$  vs.  $\nabla_x \mu_s$  plots, such as the ones shown in Fig 2. This procedure allows us to obtain  $\Gamma_{ps}$  as a function of the monomer-solute interaction strength  $\epsilon_{sm}^{LJ}$ . We stress that, whilst we determine  $\Gamma_{ps}$  by varying  $\nabla_x \mu_s$ , we keep the bulk composition of the mixture fixed (as well as the temperature and the pressure). The resulting relation between  $\epsilon_{sm}^{LJ}$  and  $\Gamma_{ps}$  is shown in Fig 3. As expected,  $\Gamma_{ps}$  is linear in  $\epsilon_{sm}^{LJ}$  when  $\epsilon_{sm}^{LJ}/\epsilon_{sf}^{LJ}$  is close to one. However, as the monomer-solute interaction gets stronger,  $\Gamma_{ps}$  saturates, and subsequently decays with increasing  $\epsilon_{sm}^{LJ}$ .

The observed decrease of  $\Gamma_{ps}$  for large values of  $\epsilon_{sm}^{LJ}$  suggests that when solute particles bind strongly to the polymer, they become effectively immobilised and hence cannot contribute to the diffusio-osmotic flow through and around the polymer. This argument would suggest that the diffusiophoretic velocity should vanish as  $\epsilon_{sm}^{LJ}$  becomes much larger than the thermal energy. However, that does not seem to be the case: rather  $\Gamma_{ps}$  seems to level off at a small but finite value. This suggests that not all fluid particles involved in the phoretic transport are tightly bound to the polymer. One obvious explanation could be that the LJ potential that we use is sufficiently long-ranged to interact with solute particles that are in the second-neighbour shell around the monomeric units of



the polymer. To test whether this is the case, we repeated the simulations with a shorter-ranged short-ranged Lennard-Jones-like potential (SRLJ) that has a smaller cut-off distance ( $r_c = 1.6$ ) where the potential and its first derivative vanish continuously. In the insert of Fig. 3 this narrower potential is shown compared with the standard truncated and shifted LJ potential with  $r_c = 2.5$ ,  $\epsilon^{LJ} = 1$  and  $\sigma^{LJ} = 1$ . In our simulations we only used the SRLJ potential for the monomer-solute interactions. For all other interactions we still use the standard LJ potential.

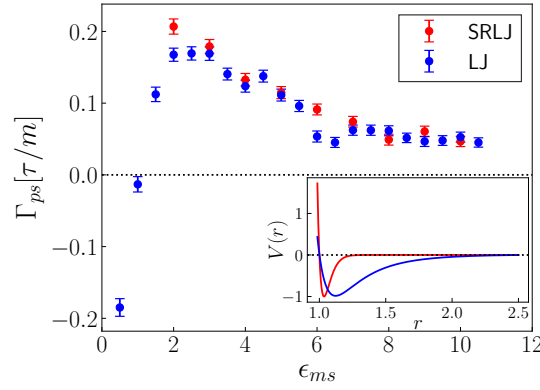


FIG. 3: Mobilities for different LJ interactions ( $\epsilon, \sigma$ ) vs the number of monomers in the polymer  $N$ . All the simulations were performed keeping the thermodynamic conditions in the bulk constant ( $T, P, c_s^B$ ). The insert shows a LJ potential for  $r_c = 2.5$ ,  $\epsilon^{LJ} = 1$  and  $\sigma^{LJ} = 1$  and a SRLJ potential, showing the narrow range of the solvent-monomer interaction.

Figure 3 shows a comparison of the results obtained with the LJ and the SRLJ potentials. Interestingly, even with the short-ranged monomer-solute interaction for which next-nearest neighbour interactions are excluded,  $\Gamma_{ps}$  still does not decay to zero at large  $\epsilon_{sm}^{LJ}$ . This suggests that the phoretic force is not just probing the excess of solute particles that are directly interacting with the polymer, but also the density modulation of solutes (and solvent) that is due to the longer-ranged structuring of the mixture around the polymer coil. In Fig. 4, we show an extreme case ( $\epsilon_{sm}^{LJ} = 8.0$ ) where the polymer has collapsed and particles within a hydrodynamic radius  $R_h$  from the center of mass do not contribute to phoresis as they are tightly bound. Contrary to what happens to particles in the structured liquid layer outside, which can be mobile and therefore generate osmotic flow.

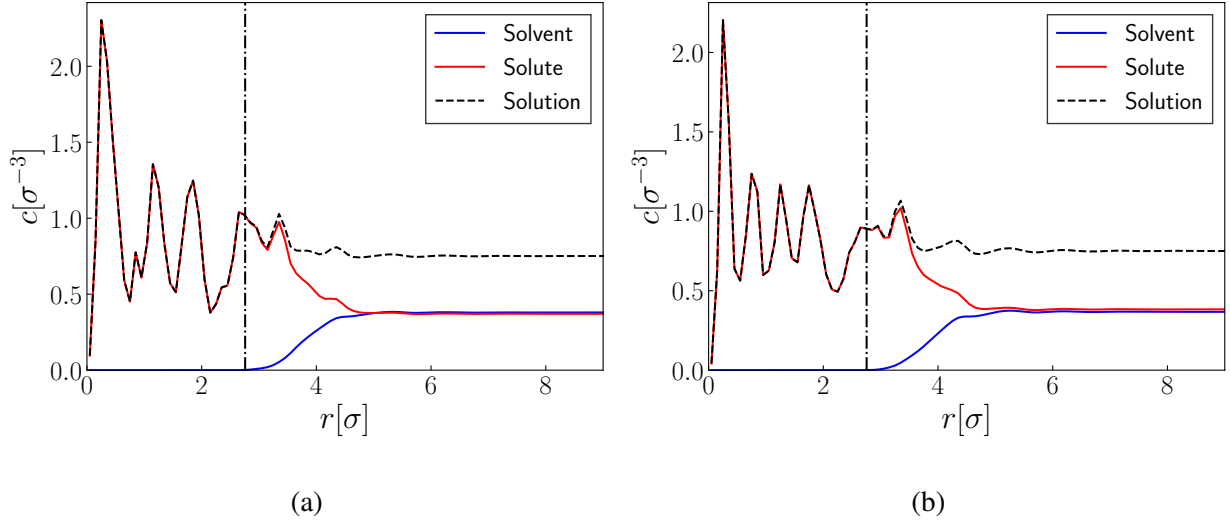


FIG. 4: Distribution of solutes, solvents and the total solution measured from the center of mass of the polymer for (a) LJ, (b) SRLJ. The vertical line represents the hydrodynamic radius  $R_h$  of the polymer, in both cases  $\varepsilon_{sm}^{LJ} = 8.0$ . Mobile particles in the heterogeneous region outside the collapsed polymer coil contribute to the diffusio-osmotic flow in a similar way for both ranges of interaction.

### C. Scaling of the phoretic mobility with the length of the polymer

For colloidal particles with a radius much larger than the range of the colloid solute interaction, the diffusiophoretic mobility is independent of the colloidal radius<sup>18</sup>. As the diffusion of a polymer in a fluid is often described as that of a colloid with an equivalent “hydrodynamic radius”  $R_h$ , one might be inclined to assume that the diffusiophoretic mobility of a sufficiently large polymer might also be size independent. To our knowledge, this size dependence has not been tested in simulations. However, experiments by Rauch and Köhler<sup>19</sup> showed that thermophoretic mobility of polymers varies with the molecular weight  $M_w$  for short polymers (fewer than 10 monomers), but very little for longer polymers (10-100 monomers).

For colloids, Anderson<sup>18</sup> derived an expression for the diffusiophoretic mobility of colloids in the case where the range  $\delta$  of colloid-solute interaction is shorter, but not much shorter than the radius  $a$  of the colloid. Introducing the small parameter  $\lambda \equiv \delta/a$ , Anderson derived the following asymptotic expression for the diffusiophoretic velocity  $U$  of a colloidal particle:

$$U = U_0 \left[ 1 - \frac{(K+H)}{\delta} \lambda + \mathcal{O}(\lambda^2) \right]. \quad (8)$$

In this approximation, the first term corresponds to the Derjaguin limit  $\delta \ll a$ :

$$U_0 = \frac{\alpha}{\beta \eta} L^* K, \quad (9)$$

where  $\alpha$  is the magnitude of the concentration gradient,  $\beta = 1/(k_B T)$ ,  $\eta$  is the shear viscosity and  $\phi$  is the potential of mean force experienced by solutes at a distance  $y = r - a$  from the surface of the colloid.

The corrections terms in Eq. (8) take into account the curvature of the particle.  $K$ ,  $L^*$ ,  $H$  are proportional to moments of the excess solute distribution  $c_s(y) = c_s^B \exp[-\beta \phi(y)]$ ,

$$K = \int_0^\infty [\exp[-\beta \phi(y)] - 1] dy, \quad (10)$$

$$L^* = \frac{\int_0^\infty y [\exp[-\beta \phi(y)] - 1] dy}{K}, \quad (11)$$

$$H = \frac{\int_0^\infty \frac{1}{2} y^2 [\exp[-\beta \phi(y)] - 1] dy}{\int_0^\infty y [\exp[-\beta \phi(y)] - 1] dy}. \quad (12)$$

All the above equations apply to the case where there is no hydrodynamic slip on the surface of the colloid. However, if solute particles are strongly adsorbed to the colloid, they become immobile and the result is simply that the surface of no slip, and hence the effective colloidal radius, increases.

To study the dependence of the phoretic motion of a polymer on the number of monomers of the chain  $N_m$ , simulations were performed for a range of  $N_m$  from 5 to 60. As our polymers are fully flexible (but self-avoiding) a chain of 60 beads corresponds to a medium-sized polymer. The simulation box was scaled accordingly with the Flory exponent for a polymer in a good solvent  $\nu \approx 0.6$  thus ensuring that the chain could not overlap with its periodic images. All the NEMD simulations were carried out for  $10^8$  time steps.

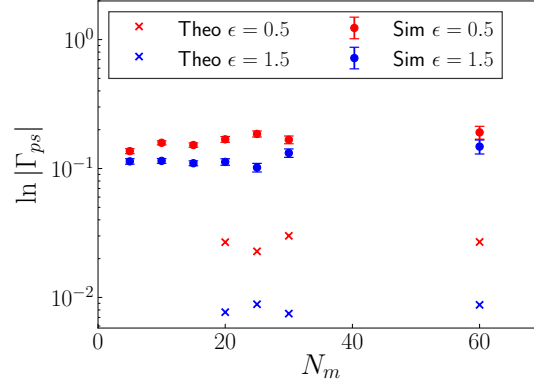


FIG. 5: Diffusio-phoretic mobilities of the polymer  $\Gamma_{ps}$  vs the number of monomers in the polymer  $N_m$ . The simulation results are shown in dots with error bars and the theoretical predictions using Eq. (8) are shown in crosses. In the theoretical calculations  $a = R_h$ , where  $R_h$  is the hydrodynamic radius estimated using Stokes-Einstein equation.

In Fig. 5, the simulation results are shown together with theoretical predictions replacing the polymer by an equivalent hard sphere with a radius  $a = R_h$ , with the hydrodynamic radius  $R_h$  given by Stokes-Einstein relation,

$$R_h \equiv \frac{k_b T}{6\pi\eta D}, \quad (13)$$

where  $\eta$  denotes the viscosity of the solution in the bulk, which was computed independently, using the Green-Kubo relation relating  $\eta$  to the stress auto-correlation function, in an equilibrium simulation of the bulk fluid (see, e.g.<sup>20</sup>). The diffusion coefficient  $D$  was also computed from equilibrium simulations<sup>21</sup>. Fig. 5 shows that the diffusio-phoretic mobility of the polymer increases with  $N_m$ . The large quantitative differences between the simulations and the theoretical approximations for a colloid with the same hydrodynamic radius are to be expected: First of all, the assumption that the polymer coil behaves as a hard sphere with  $a = R_h$  is rather drastic. To be more precise, this approximation (that was also used by Kirkwood<sup>22</sup>) assumes that the liquid molecules within the coil region move together, such that the whole assembly moves as a rigid sphere (see e.g.<sup>23</sup>). This might be a good approximation for the diffusion of long polymer coils, but in the case of phoresis, it is unrealistic to assume that no solute/solvent can be transported through the polymer at distances less than  $R_h$ . The second (but related) questionable approximation is that  $R_h$  defines the surface of the equivalent colloid in the integrals in Eqs. (10)-(12). As a consequence, the contribution of any excess solute at a distance less than  $R_h$  from the polymer center is ignored. As is clear from Fig. 4 this assumption is incorrect and is likely to underestimate

the real diffusio-phoretic flow, in view of the fact that Fig. 6b shows that there can be considerable solute advection for  $r < R_h$ . Our simulations suggest that better theoretical models for polymer diffusiophoresis are needed.

In Fig. 6 we show the velocity field for a polymer with  $N_m = 30$  for two cases: 1) when it is subjected to a body force i.e pressure gradient 6a and 2) under the influence of diffusiophoresis 6b. As is obvious from the figure, in both cases there is fluid motion within the polymer at distances less than  $R_h$  from its center of mass. However, there is an important difference between the flows inside the polymer for the pressure-driven and phoretically driven flows: strong hydrodynamic screening is found in the case of a pressure gradient while for diffusiophoresis, screening seems to be effectively absent.

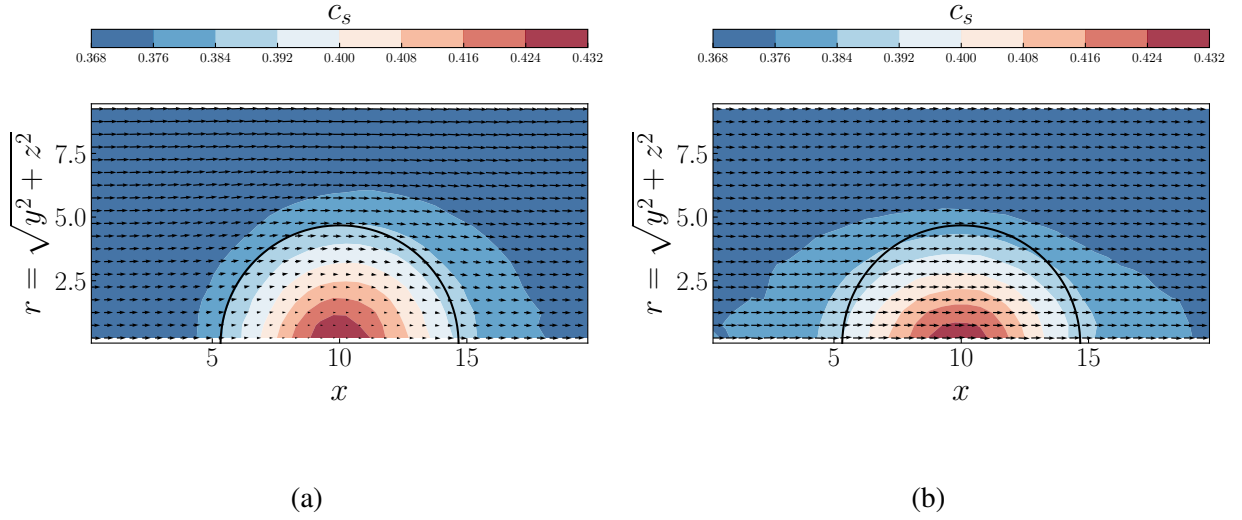


FIG. 6: Flow around a polymer coil when a body force is applied (a) and for the diffusiophoretic-case (b). The velocity field is measured in a coordinate system moving with the center of mass of the polymer. The black semicircle shows the equivalent colloid and the contours show the solute concentration, for both cases  $\epsilon_{ms} = 1.5$ . The measurements were taken inside a cylinder with axis along the direction of the applied force passing through the center of mass of the polymer. The contours show the solute concentration  $c_s$ .

## V. CONCLUSIONS

We have performed molecular dynamics simulation on the diffusiophoresis of polymers in a fluid mixture under the influence of a concentration gradient of solutes. In our non-equilibrium molecular dynamics simulation, we mimicked the effect of an explicit concentration gradient in the system by imposing equivalent microscopic forces on the solute, solvent and monomers. This approach allows us to use periodic boundary conditions and facilitates a systematic investigation of diffusiophoresis. Our results reveal a non-monotonic relation between the diffusiophoretic mobility and the interaction strength between the polymer and the solute. The findings imply that, in the strong interaction regime, the phoretic mobility decreases with increasing solute-monomer interaction strength. This result can be understood by noting that solutes that are strongly bound to the polymer cannot contribute to diffusiophoresis. Furthermore, we have demonstrated that the diffusiophoretic mobility of a (short) polymer cannot be explained in terms of a model that assumes that polymers behave like colloids with the same hydrodynamic radius. Finally, we found effectively no screening of hydrodynamic flow inside a polymer moving due to diffusiophoresis, as opposed to what is observed in the case of a polymer that is moved through a fluid by an external force.

## VI. ACKNOWLEDGEMENTS

This work was supported by the European Union Grant No. 674979 [NANOTRANS]. DF and LB acknowledge support from the Horizon 2020 program through 766972-FET-OPEN-NANOPHLOW. We would like to thank Richard P. Sear, Raman Ganti, Stephen Cox and Xipeng Wang for the illuminating discussions.

## REFERENCES

- <sup>1</sup>J. L. Anderson and D. C. Prieve, *Separation and Purification Methods* **13**, 67 (1984).
- <sup>2</sup>B. V. Derjaguin, G. P. Sidorenkov, E. A. Zubashchenkov, and E. V. Kiseleva, *Kolloidn. zh* **9**, 335 (1947).
- <sup>3</sup>B. Derjaguin, N. Churaev, and V. Muller, *Surface Forces* (Springer Science+Business Media, LLC, 1987) p. 398.
- <sup>4</sup>N. Clisby, B. Duenweg, and B. Dünweg, *Physical Review E* **94**, 052102 (2016).

- <sup>5</sup>J. Palacci, B. Abécassis, C. Cottin-Bizonne, C. Ybert, and L. Bocquet, *Physical Review Letters* **104**, 138302 (2010).
- <sup>6</sup>J. Palacci, C. Cottin-Bizonne, C. Ybert, and L. Bocquet, *Soft Matter* **8**, 980 (2012).
- <sup>7</sup>A. P. Thompson and G. S. Heffelfinger, *The Journal of Chemical Physics* **110**, 10693 (1999).
- <sup>8</sup>H. Yoshida, S. Marbach, and L. Bocquet, *Journal of Chemical Physics* **146**, 194702 (2017).
- <sup>9</sup>Y. Liu, R. Ganti, and D. Frenkel, *Journal of Physics Condensed Matter* **30**, 205002 (2018).
- <sup>10</sup>D. J. Evans and G. Morriss, *Statistical Mechanics of Nonequilibrium Liquids*, 2nd ed. (Cambridge University Press, 2008).
- <sup>11</sup>G. Ciccotti, G. Jacucci, and I. R. McDonald, *Journal of Statistical Physics* **21**, 1 (1979).
- <sup>12</sup>A. Ajdari and L. Bocquet, *Physical Review Letters* **96**, 186102 (2006).
- <sup>13</sup>S. Plimpton, *Journal of Computational Physics* **117**, 1 (1995).
- <sup>14</sup>J. D. Weeks, D. Chandler, and H. C. Andersen, *Journal of Chemical Physics* **54**, 5237 (1971).
- <sup>15</sup>M. Bishop, M. H. Kalos, and H. L. Frisch, *Journal of Chemical Physics* **70**, 1299 (1979).
- <sup>16</sup>B. Dünweg and K. Kremer, *The Journal of Chemical Physics* **99**, 6983 (1993).
- <sup>17</sup>W. G. Hoover, *Physical Review A* **31**, 1695 (1985).
- <sup>18</sup>J. L. Anderson, M. E. Lowell, and D. C. Prieve, *Journal of Fluid Mechanics* **117**, 107 (1982).
- <sup>19</sup>J. Rauch and W. Köhler, *Macromolecules* **38**, 3571 (2005).
- <sup>20</sup>J. P. Hansen and I. R. McDonald, *Theory of simple liquids*, 3rd ed. (Academic Press, 2006).
- <sup>21</sup>D. Frenkel and B. Smit, *Academic, New York*, 2nd ed. (Academic Press, 2002).
- <sup>22</sup>J. G. Kirkwood, *Journal of Polymer Science* **12**, 1 (1954).
- <sup>23</sup>G. Strobl, *The Physics of Polymers: Concepts for Understanding their Structure and Behavior*, 3rd ed. (Springer-Verlag, 2007).